3D NUMERICAL SIMULATION OF EDDY CURRENT TESTING OF A BLOCK WITH A CRACK

Toshiyuki Takagi, Mitsuo Hashimoto, Toshihiko Sugiura,
So Norimatsu, Seiji Arita, and Kenzo Miya

Nuclear Engineering Research Laboratory
The Faculty of Engineering, The University of Tokyo
Tokai, Ibaraki 319-11, Japan

INTRODUCTION

There are many approaches to 3D eddy current analysis. Typical methods for the eddy current analysis are the A-ϕ method and the T-ω method. Both methods require variables in space as well as in a conductor. We have already proposed the T method [1, 2, 3], where a magnetic scalar potential ω is not included and we do not need variables in space. But the method has a disadvantage that a large core memory is needed due to a dense matrix.

TEAM (Testing Electromagnetics Analysis Method) workshop [4] is now going. The objectives of the TEAM workshop are to compare the numerical results solved by many computer codes and to verify the modelings, numerical techniques, and computer codes. One of the TEAM workshop problems is an ECT(eddy current testing) problem.

The ECT is a type of non-destructive testing and effective for detecting surface cracks or flaws in conductive materials. Since this phenomena is 3D in nature, 3D numerical analysis of eddy current is required in order to know eddy current distribution in the conductor and to improve the ECT technique. It is now well understood that the numerical analysis plays the very important role for the solution of both forward and inverse ECT [5].

The purposes of this paper are as follows:

(1) Development of practical eddy current analysis method using T method
(2) Measurement of signal trajectories for ECT of a block with a crack (TEAM problem No.8)
(3) Application of the method to the ECT problems and the verification of the method

Review of Progress in Quantitative Nondestructive Evaluation, Vol. 9
Edited by D.O. Thompson and D.E. Chimenti
Plenum Press, New York, 1990

METHOD

Basic Equations

The following two of four Maxwell equations are enough to determine transient distribution of eddy current.

Ampere's law

$$\nabla \times \vec{H} = \vec{J} \tag{1}$$

where $\vec{H}$ and $\vec{J}$ are magnetic field and current density vectors.

Faraday's law

$$\nabla \times \vec{E} = -(\frac{\partial \vec{B}_e}{\partial t} + \frac{\partial \vec{B}_o}{\partial t}) \tag{2}$$

where $\vec{B}_e$ and $\vec{B}_o$ are induced and applied magnetic induction vectors.

These equations are supplemented with the following constitutive equations.

$$\vec{B} = \mu_o \vec{H} \tag{3}$$

$$\vec{J} = \sigma \vec{E} \tag{4}$$

where μ_o and σ are magnetic permeability of air and electrical conductivity.

Since displacement current is neglected in eq.(1), conservation of current($\nabla \cdot \vec{J} = 0$) is secured. Thus current vector potential, T, is defined as,

$$\vec{J} = \nabla \times \vec{T}. \tag{5}$$

Biot-Savart's law is written,

$$\vec{B}_e = \frac{\mu_o}{4\pi} \int_v \vec{J}' \times \nabla' \frac{1}{R} dV'. \tag{6}$$

After the very lengthy calculation the relation between induced magnetic induction and the current vector potential is given as the following equation.

$$\vec{B}_e = \mu_o \vec{T} + \frac{\mu_o}{4\pi} \int_s T_n' \nabla' \frac{1}{R} dS' \tag{7}$$

Governing Equations of T-Method

Introducing eq.(7) into eq.(2) and using eqs.(4) and (5), we obtain the governing equation for the eddy current analysis.

$$\nabla \times \frac{1}{\sigma} \nabla \times \vec{T} + \mu_o \frac{\partial \vec{T}}{\partial t} + \frac{\mu_o}{4\pi} \int_s \frac{\partial T_n'}{\partial t} \nabla' \frac{1}{R} dS' + \frac{\partial \vec{B}_o}{\partial t} = \vec{0} \tag{8}$$

In this paper we deal with an AC problem. Eq.(8) is rewritten using imaginary unit, j, and angular frequency, ω.

$$\nabla \times \frac{1}{\sigma}\nabla \times \vec{T} + j\omega\mu_o\vec{T} + j\omega\frac{\mu_o}{4\pi}\int_s T_n'\nabla'\frac{1}{R}dS' + j\omega\vec{B}_o = \vec{0} \tag{9}$$

We solve eq.(9) with the gage condition eq.(10) and the boundary condition eq.(11) using the finite element method.

Gauge condition

$$\nabla \cdot \vec{T} = 0 \tag{10}$$

Boundary condition on conductor surface

$$\vec{T} \times \vec{n} = \vec{0} \tag{11}$$

We can summarize advantages of T-Method as follows:

(1)There is only one variable (one vector with three components).
(2)No variables exist in space.
(3)It is easy to treat external current and field.

Matrix Equation Using Iterative Solution Technique [3]

The Galerkin method is applied to eq.(9). The obtained coefficient matrix is complex, asymmetric and dense. Direct matrix equation solution procedures such as Gaussian elimination have been commonly used. In this iteration technique developed here, we split the matrix into two matrices. One matrix corresponds to the first and second terms of eq.(9). It is complex, symmetric, and banded. The other corresponds to the third, "non-local term". It is imaginary, asymmetric, and almost dense. An (i,j) component of the matrix is not equal to zero when j corresponds to normal components of surface nodes.

The iterative method is proposed where the current vector potential in the n-th iteration can be obtained as the solution of the following equation.

$$[P]\left\{T^{(n)}\right\} = \left\{f^{(n)}\right\} \tag{12}$$

where

$$\left\{f^{(n)}\right\} = \alpha\left[\{B_o\} - [Q]\left\{T^{(n-1)}\right\}\right] + (1-\alpha)\left\{f^{(n-1)}\right\} \tag{13}$$

α : relaxation factor
(n) : n-th iteration
$[P]$: Complex, symmetric, band matrix
$[Q]$: Imaginary, unsymmetric, dense matrix

Iteration technique converges when the spectral radius of the iteration matrix is less than one[6].

Iteration matrix

$$-\alpha[P]^{-1}[Q] + (1-\alpha)I \tag{14}$$

Spectral radius

$$\rho = Max \mid \lambda_i \mid < 1 \tag{15}$$

$$\lambda_i = -\alpha (p_i + jq_i) + (1 - \alpha) \tag{16}$$

where $p_i + jq_i$ is an eigenvalue of $[P]^{-1}[Q]$.

EXPERIMENT

As an ECT problem, we adopted the standard one proposed in the TEAM workshops for eddy current code comparison [4] and also presented in some papers [7, 8]. The test piece is a rectangular block 330x285x30mm with a 40x0.5x10mm flaw on the center of one of the larger faces, as shown in Fig.1. It is made of austenitic steel type 18-10 Mo with less than 2% of ferrite. Relative permeability μ_r is 1 and conductivity σ is $0.14 \times 10^7 S/m$(Siemens per meter).

A differential probe moves on the surface of the block (Fig.2). The probe is a cylinder with an induction solenoid and two smaller reception solenoids. By moving the probe, we can obtain a signal trajectory which corresponds to the image on the complex plane of the difference of magnetic fluxes through the two reception solenoids.

In our experiment, the probe was fixed and the block was moved using an X-Y table. The probe is connected to a conventional ECT equipment which supplies AC current to an induction solenoid and displays output signals from the reception solenoids on a cathodic screen. The experiments were carried out for 2 different movements of the probe (parallel and perpendicular to the plane of the flaw).

NUMERICAL ANALYSIS

Numerical analysis was also carried out for the same problem. For the symmetry the region to be meshed is only a half of the block. The flaw is treated as a low conductive region and included in the analysis

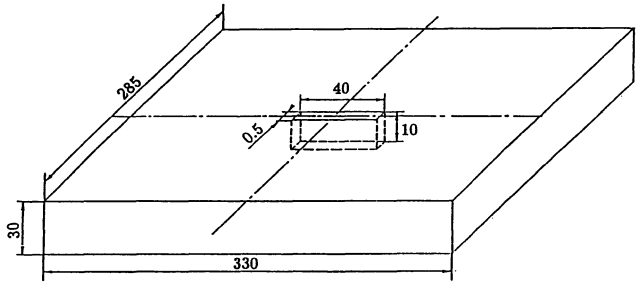

conductivity : $\sigma = 1.4 \times 10^6\ s/m$
relative permeability : $\mu_r = 1$
frequency : $f = 500Hz$

Fig.1 The Block with a flaw as NDT model.

Table 1 Core memory and CPU time

Nodes	1169
Elements	200
Nodes on surface	662
Elements on surface	180
Unknowns	3507
Half band width	387
Computer	S820
Core memory (Mbyte)	76
CPU time (sec)	
① Matrix generation	100
② LU decomposition	5
③ Back substitution	52
④ flux calculation	80
⑤ total	237

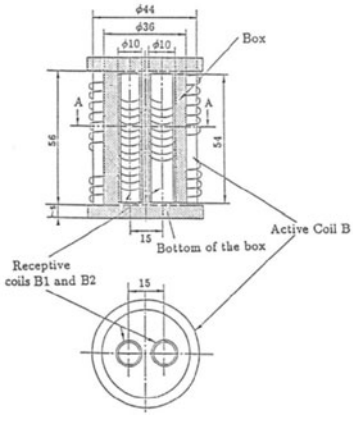

Fig.2 Configuration of the probe.

domain. The conductivity was assumed $5.0 \times 10^2 S/m$, which is low enough compared to that of the block.

Fig.3 shows one example of mesh division when the coil moves parallel to the flaw. Table 1 gives the number of nodes, elements, unknowns, memory and CPU time. We used a HITAC S-820 supercomputer.

Fig.4 shows eddy current distribution on the top surface when the coil locates at x=80 mm. One can see that eddy current distributes locally near the coil and current is very small a t a location more than 100 mm distant from the coil.

This fact gives us an idea that regions near the coil should be divided into fine meshes though far region need not be. In this problem the coil moves from x=0 to x=80mm, thus, to solve this whole problem with one pattern of mesh division requires too many elements under the present memory limitations. Therefore, according to each coil position, we used a different type of mesh division in the x direction, as shown in Fig.5.

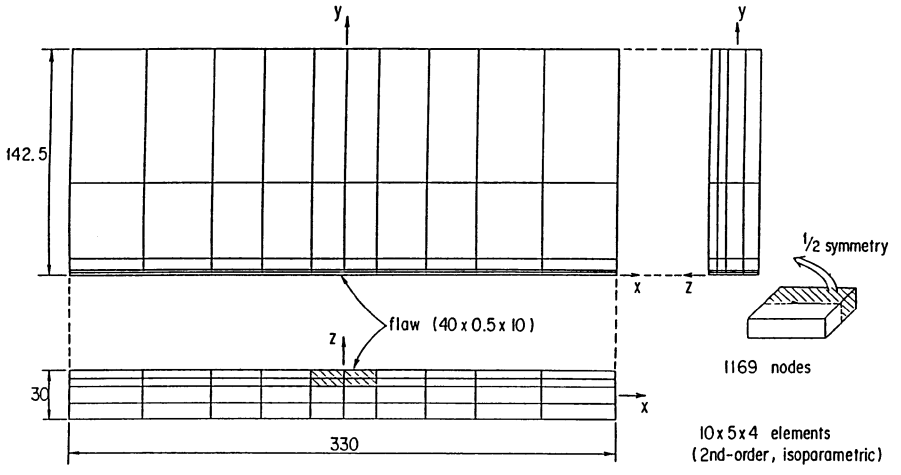

Fig.3 Mesh division for NDT probe.

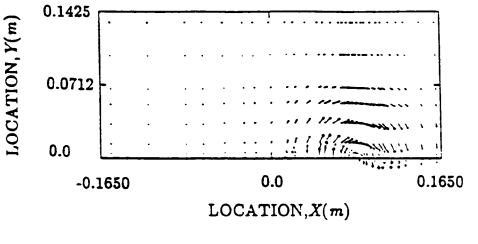

(a) Real Part

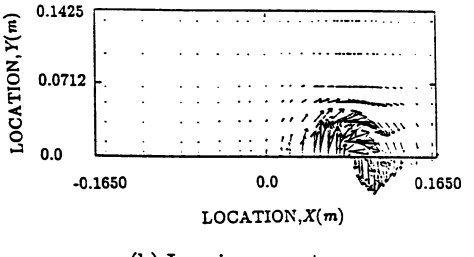

(b) Imaginary part

Fig.4 Eddy current distribution on top surface. (Coil : X=80mm, Y=0mm)

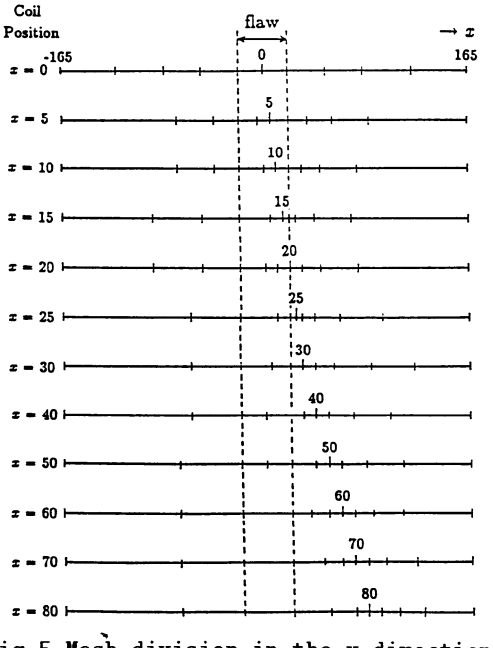

Fig.5 Mesh division in the x direction according to each coil position.

In each coil location, at first the matrix of the system is built, and then solution of current vector potential is obtained with the iterative technique. Next, the flux of the induced field is calculated through the two reception solenoids and the difference between them gives a point of the output signal. After the calculation at all coil locations, connecting these signal points indicates the signal trajectory.

RESULTS AND DISCUSSIONS

Figs.6 and 7 show the numerical and experimental results for a coil movement parallel and perpendicular to the flaw when the frequency is 500Hz. Results show almost good agreement both in shape and phase angle.

One reason for the discrepancy may be lack of accuracy in both the numerical simulation and the experiment. The output signal here is the difference of fluxes through the two solenoids which are very close to each other. Therefore, from numerical point of view, it requires higher accuracy, compared with current vector potential. And the number of meshes, especially for the region near the coil, may not yet be enough to achieve the accuracy. From the experimental side, there are some deficiencies in the electrical specification of the coil so

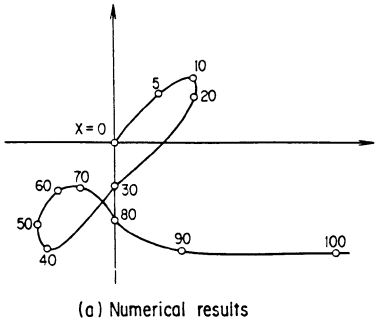

(a) Numerical results

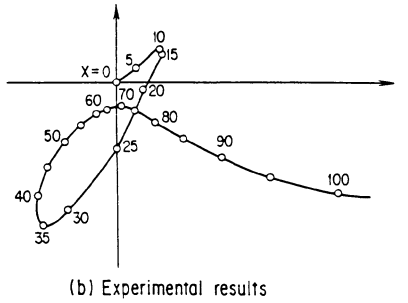

(b) Experimental results

Fig.6 Comparison between numerical and experimental results. (f=500Hz, parallel to the flaw)

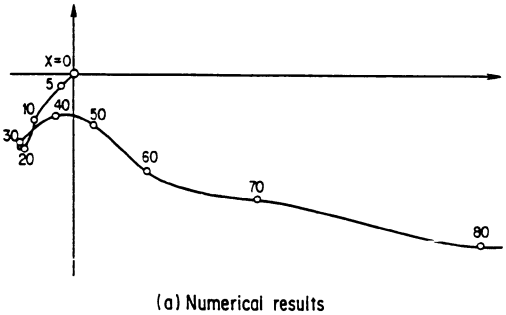

(a) Numerical results

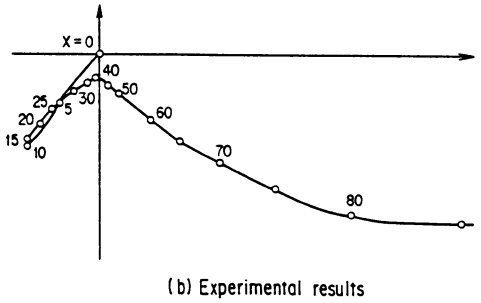

(b) Experimental results

Fig.7 Comparison between numerical and experimental results. (f=500Hz, perpendicular to the flaw)

that there may be a low sensitivity problem especially when the frequency is low.

Second reason may be the disagreement of the wave form in the numerical analysis and the experiment. The AC current supplied to the inducting solenoid by ECT equipment is a triangular wave while in the numerical analysis we use a sine wave. The triangular wave includes higher frequency component, which may affect the signal trajectory.

CONCLUSIONS

1. A numerical technique for 3D eddy current analysis using a current vector potential (T) method and an iterative solution technique was successfully developed. In this technique mesh division was adapted to the position of coils and a flaw.

2. Signal trajectories for ECT of a block with a crack were measured. An experiment was performed for a benchmark problem of TEAM workshop.

3. The method was applied to the ECT problem. Numerical results for 500Hz agreed with measured values in some important features. CPU time and main memory were 4 minutes and 76 Mbytes.

REFERENCES

1. K. Miya et al., Proceedings of the IUTAM Symposium, Tokyo, October, 1986, North-Holland, pp.183-189.
2. K. Miya and H. Hashizume, IEEE Transactions on Magnetics, Vol.24, pp.134-137, January 1988.
3. T. Takagi et al., IEEE Transactions on Magnetics, Vol.24, No.6, pp.2682-2684, November 1988.
4. L.R. Turner, TEAM Test problems, ANL, April 1988.
5. W. Lord, Applied Electromagnetics in Materials, Pergamon Press, pp.117-125, 1989.
6. R.S.Varga, Matrix Iterative Analysis, Presentice-Hall, Inc., 1962.
7. J.C. Verite, COMPEL, Vol.13, pp.167-178, 1984.
8. A. Bossavit and J.C. Verite, IEEE Transactions on Magnetics, Vol.19, pp.2465-2470, November 1983.